In Vitro and In Vivo Evaluation of Osteoconductive Properties of Novel GelMa/Eggshell-Derived Calcium Phosphate Composite Scaffold

Jodal Mohammedamim Ahmed[1*], Shehab Ahmed Hamad[2]

Jodal Mohammedamim Ahmed[1*], Shehab Ahmed Hamad[2]
[1]BDS., MSc., Department of Oral and Maxillofacial Surgery, College of Dentistry, Hawler Medical University, Erbil, Iraq
[2]BDS, MSc, MOMSRCPS (Glasg), FICMS,FICD, FFDRCSI (OSOM), FDSRCPS (Glasg), FDSRCSEng, Department of oral and maxillofacial surgery Department, collage of Dentistry, Hawler Medical University, Erbil, Iraq

Correspondence:
Jodal Mohammedamim Ahmed
BDS., MSc., Department of Oral and Maxillofacial Surgery, College of Dentistry, Hawler Medical University, Erbil, Iraq
Email: Jodal.ahmed@hum.edu.krd

History:

- Received: March 23, 2020
- Accepted: June 17, 2020
- Published: Sept 2, 2020

DOI: https://doi.org/10.31838/ejmcm.07.02.01

ABSTRACT

GelMa/ES-HA composite scaffold was sucessfully fabricated via freeze-drying process. The cytotoxicity of composite scaffolds was low after 24 h incubations (The viability of cells was above 85%). However, the cell viability decreased over time (71.9% after 48 h and 60.0% after 72 h). ALP activity of the cells grown on scaffold samples was significantly higher than that of polystyrene plates under the same condition ($p < 0.05$). Also, ALP activity of scaffold samples increased over time. Osteocalcin synthesis for the cells cultured on the GelMa/ES-HA scaffold was significantly higher than on the polystyrene plate after 6 days of culture. The results of ALP activity and osteocalcin synthesis suggest that the bioactive GelMa/ES-HA scaffold improved the development of a mature osteoblast phenotype. SEM micrographs of the HOS cells grown on the scaffold after culturing for 3 days confirmed the favorable cells growth of cells on the surface of scaffold or between its pores and also formation of calcium deposits.

The histological examination of bone sections showed deposition of osteoid bone in all studied groups after 1-week and immature bone spicules rimmed by osteoblasts were observed more clearly in treatment groups. Significant osteoid matrix synthesis and mineralization accelerated was by early cell differentiation. The number of osteocytes and osteoblasts as mean values increased during the transition from the 1, 4 to 8 and 12-weeks of healing intervals among treatment groups. While, the Osteoclast population in treatment groups decreased over time. The production of Osteocalsin, Osteopointin and Osteronectin in treatment groups significantly increased over time ($p < 0.05$). Furthermore, the difference between Osteocalsin, Osteopointin and Osteonectin production in all treatment group and control groups was significant ($p < 0.05$) except for the 1 week groups. The maximum Osteocalsin, Osteopointin and Osteronectin production belonged to 3 months treatment group which were 34.26, 42.43 and 34.26, respectively; which this values for 3 months control groups were 17.49, 14.73 and 14.50.

The results of this study showed that the novel GelMa/ES-HA composite scaffold is a bioactive, biocompatible, biodegradable bone graft with desired mechanical and swelling properties and excellent potential for enhancing bone regeneration process which could serve as a promissing candidate for bone and dental tissue engineering applications.

Keywords: Egg shell-derived Hydroxyapatite; GelMA; Freeze Drying; Tissue Engineering; *In vitro; In vivo.*

INTRODUCTION

Tissue engineering techniques have been employed to restore the function of damaged tissues and organs. In most cases, tissue engineering techniques for many applications such as cell culture, tissue transplantation and tissue regeneration are separated from scaffolds that have different structures, properties and functions [1,2]. Scaffolds can therefore play a very effective role in tissue engineering applications by providing optimal 3D space for the proper transport of nutrients and metabolites for the purpose of tissue organization. Extracellular matrix molecules or ECMs including fibronectin, laminin, and their cell surface glycoprotein receptors are involved in cell migration and differentiation. In fact, ECM components form the basis of tissue engineering. Cell dynamics play an important role in facilitating and organizing many cellular processes. In addition to the role of scaffolding and attachment for cells, the ECM also helps to prepare and isolate the growth factors needed for cells. One of the main functions of a tissue engineering scaffold is to replicate ECM [3-5].

The importance of using scaffolds in optimizing, remodeling and repairing the target tissue is that the primary cells implanted in the scaffolding begin to divide and fill the implantation area. Binding factors that accumulate inside the scaffold environment increase cell attachment and migration, thereby reducing the recovery time and duration of the period [6-8]. Careful control of the scaffold structure minimizes side effects such as inflammation and early enzymatic degradation. Due to the degradability of these substances, they are no longer required to be removed in transplant or fetal patients. This removal should be performed by a re-operation on the patient, which eliminates the secondary surgery by using these degradable substances, making the patient more comfortable and cost effective. These scaffolds are not toxic to the body and do not lead to an immune response in the recipient and are compatible with living tissue [9-11.

So far scaffolds have been extensively developed through the use of natural and synthetic biodegradable polymers. Most of the synthetic polymers associated with tissue engineering include polylactide, polyglycolide, poly caprolactone and their copolymers [11-14]. These synthetic polymers employed have many obvious drawbacks, such as slow degradation, hydrophobicity, production of acidic degradation products, and lack of cell diagnostic sites.

Therefore, many natural polymers have been chosen as substitutes for scaffolds [15-17].

Gelatin methacrylate or GelMa is gelatin-based polymer, which has recently been widely used in medical engineering applications including tissue engineering and scaffolding, drug release and biosensors, due to its good biocompatibility and degradability [18-22]. GelMa can be prepared from the reaction of gelatin and methacrylic anhydride in a neutral medium at 50 °C. After dilution and dialysis, the gel is eventually freeze and dried. In order to create hydrogels and crosslink the polymer chains, primers and UV radiation is required. Conventional initiators include lithium acyl phosphinate. The concentration of gel and primer in solution and the amount of ultraviolet radiation are the main factors in the regulation of hydrogel properties [18]. Besides the biocompatibility and biodegradability properties of this material, composites can achieve other desirable properties such as conductivity and mechanical properties. The application of hydrogel-based composites because of their unique properties provides a promising future for the application of these materials in medical engineering [23-25]. Therefore, we aim to fabricate a composite scaffold of GelMA hydrogel and egg shell derived hydroxyapatite.

Calcium carbonate (calcite) is the main component in eggshells and is the major inorganic substance found in an egg and it makes up about 94% of chemical composition of eggshell. This makes it an essential material for hydroxyapatite production [26-27].

In this study, the aim is to evaluate the osteoconductive properties of GelMA/egg-shell hydroxyapatite composite scaffold via *in vitro* and *in vivo* evaluations. The analyses are performed in terms of osteonectin, osteopontin and osteocalcin production, ALP activity, cell count and histopathological analysis.

MATERIALS AND METHODS

2.1 Materials

PBS solution, RPMI, MTT, Dulbecco's modified Eagle's medium (DMEM), Dimethyl sulfoxide, Glycine, NaOH, p-nitrophenol phosphate buffer (PNPP), Lanthanum chloride, HCL were provided from Sigma Aldrich, USA). Phosphoric acid and Methacrylic anhydride were purchased from Merck Millipore, Germany). Triton X-100 was obtained from Gibco, Grand Island, NY. L929 human fibroblasts and OSTEOBLAST-LIKE HOS Osteoblast cells were provided from Genetic Research Institute, Tehran, Iran.

2.2 Methods

The GelMA/egg-shell HA composite scaffolds from our previous study were prepared in the form of cylinder with the diameter of 8 mm and height of 6 mm, and the average porosity of 250 nm.

2.2.1 In vitro Studies

2.2.1.1 Cytotoxicity Assay

MTT assay was used to evaluate the viability of L929 human fibroblasts (Genetic Research Institute, Tehran, Iran) in the presence of composite scaffolds. To do so, cells were seeded into a 96-well microplate containing composite scaffolds at the density of 1×10^4 cell/scafolld and stored in RPMI medium, 37 °C, and humid atmosphere containing 5% carbon dioxide. The control sample was the cells cultured with fresh medium. Twenty-four, 48 and 72 hours after incubation, 10 µl of MTT solution (5 mg / ml) was added to each well and kept in the incubator again for 4 hours. MTT solution in living cells were transformed into formazan crystals, which were then dissolved in dimethyl sulfoxide creating a purple color. The optical density (OD) at 570 nm was measured by a microplate reader. The relative cytotoxicity was calculated as follows:

$$Cytotoxicity = (1 - \frac{a_t}{a_c}) \times 100 \qquad (1)$$

Where, a_t is the OD of treated cells and a_c is OD of cells in the control group.

2.2.1.2 Alkaline phosphatase activity

Two main markers of osteoblastic differentiation are alkaline phosphatase and osteocalcin. Alkaline phosphatase expression of OSTEOBLAST-LIKE HOS osteoblasts was determined spectrophotometrically. The scaffold samples were autoclaved and then placed in 400 mL serum-free, sterile Dulbecco's modified Eagle's medium (DMEM) (Gibco, Grand Island, NY) for 24 h. The samples were seeded with 1×10^5 OSTEOBLAST-LIKE HOS Osteoblast cells (100 lL) and incubated at 37 °C for 60 min. Then, 2 ml DMEM containing the nutrient F-12 medium (DMEM/F12; Gibco, Gaithersburg, MD) supplemented with penicillin-streptomycin and 10% heat-inactivated FBS was added to the samples. The cells seeded directly on the polystyrene plates were considered as control. The medium was changed every day until day 6. Then, the cells were harvested and the medium were removed and washed twice with PBS. The cells were detached from the samples by trypsinization.

The detached Cells were lysed and mixed with 0.1 ml 0.1 M glycine/NaOH buffer (pH 10.2), 0.1 ml 15 mM *p*-nitrophenol phosphate (PNPP), 0.1 ml 0.1% (v/v) Triton X-100 in saline and 0.1 ml double distilled water. Each supernatant was incubated at 37 °C for 30 min and then 2.5 ml 1 M NaOH was added to each supernatant, and these were placed in ice to stop the enzyme reaction. The production of *p*-Nitrophenol (PNP) by alkaline phosphatase in the lysate cell was estimated by measuring the absorption at 410 nm. The slope of the absorbance versus time plot was used to calculate the enzyme activity.

2.2.1.3 Osteocalcin production

To determine the amount of calcium deposits in the cell seeded scaffolds, they were hydrolyzed with 6 M HCL and then diluted with 0.5% (v/v) lanthanum chloride. The amount of calcium was measured by atomic absorption spectroscopy.

2.2.2. In vivo Studies

1 mature male Sheep weighting a mean 75 Kg and with mean age 3-4 years was obtained from Animal house-college of medicine, Hawler medical university. After sedation and

followed by giving local anesthesia to the lateral side of the Pelvic bone of the sheep, the surgical fields was shaved carefully then sterilized by beta dine (Povidine, iodine).

With a blade no.15 full-thickness incision will be made through the lateral side of the pelvic bone. The bone deficits were created according to standard practice. Using an Implant engine motor with trephine drills, the beds were prepared to produce holes of 8 mm in diameter and 4 mm depth the. The placement of the scaffolds was carried out according to standard practice.

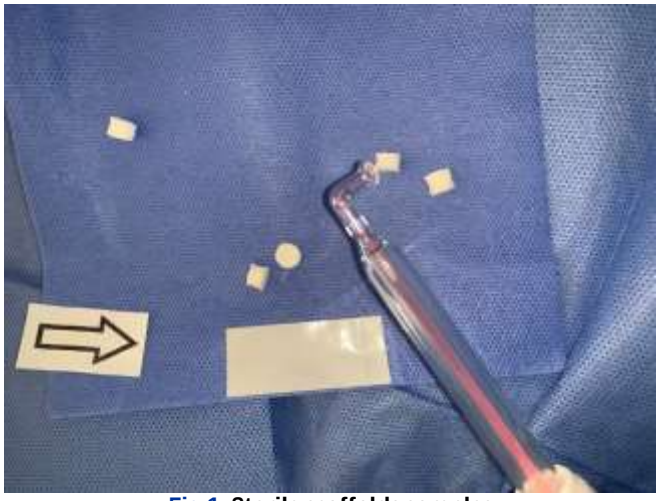

Fig 1: Sterile scaffolds samples

Fig 2: Implantation of scaffolds

Then the muscle tissue was replaced and sutured with Vicryl in continuous suture (Ethicon, Sa˜o Jose´ dos Campos, SP, Brazil), and the superficial suture including the skin performed with vicryle 4-0 suture. The operated surface was disinfected with iodine. This process was carried out in one side of pelvic bone: So that in group A: 4 scaffolds were placed in pelvic bone, and group B: 4 surgical defects was done without placement anything.

2.2.2.1 Histology and histomorphometry

After 3 months of healing, the animals were killed under general anesthesia, as described previously. The calvaria was removed and immediately fixed in buffered 10% formaldehyde solution. After fixing, the specimens were demineralized for 5 days. For paraffin embedding, each defect then separate into two halves and included in the same block. From each level, two glass microscope slides containing two or three sections were prepared. Histological sections were stained with hematoxilin and eosin.

In order to classify the stages of bone regeneration process in the H&E image of each group, the following scoring system was used: Score 1: Fibrous tissue; Score 2: Mainly fibrous + small cartilage tissue; Score 3: Fibrous tissue + Cartilage tissue equally; Score 4: Cartilage tissue ; Score 5: Mainly cartilage tissue + immature bone; Score 6: Cartilage tissue + immature bone equally; Score 7: Immature bone + small cartilage tissue; Score 8: Immature bone; Score 9: Immature bone +mature bone; Score 10: Mature bone.

2.2.3 Statistical analysis and data management

Statistical significance was determined using t-test (SPSS 24). P-values < 0.05 were considered statistically significant. The experiments were repeated at least three times, and the data are expressed as the mean ± standard deviation.

RESULTS AND DISCUSSION

3.1 In vitro studies

3.1.1 Biocompatibility test

To determine the biocompatibility of composite scaffolds, the viability of L929 human fibroblasts while incubating with the scaffolds for 24, 48 and 72 hours was evaluated (Fig. 3). The cytotoxicity of composite scaffolds was low after 24 h incubations (The viability of cells was above 85%). However, the cell viability decreased over time (71.9% after 48 h and 60.0% after 72 h) which could be attributed to due to the lack of mass transfer in vitro, so the byproduct of scaffold remains in the culture medium and decreases the availability of nutrients and oxygen for the cells. Also the decrease in the proliferation of cells incubated with scaffolds could be because of the quite rough morphology of scaffolds due to the presence of HA particles. Several studies have reported that surface roughness could affect cell proliferation and migration rate. However, the desirable proliferation and high levels of viability of cells on the composite scaffold confirmed their good biocompatibility. Our result was in agreement with a study by Fares et al. [28]. They also showed that IPN GelMA and pectin-g-PCL hydrogels were cytocompatible *in vitro* and could support the growth of three-dimensionally (3D) encapsulated MC3T3-E1 preosteoblasts *in vitro*. The simplicity, technical feasibility, low cost, tunable mechanical properties, and cytocompatibility of the engineered semi-IPN and IPN hydrogels highlight their potential for different tissue engineering and biomedical applications.

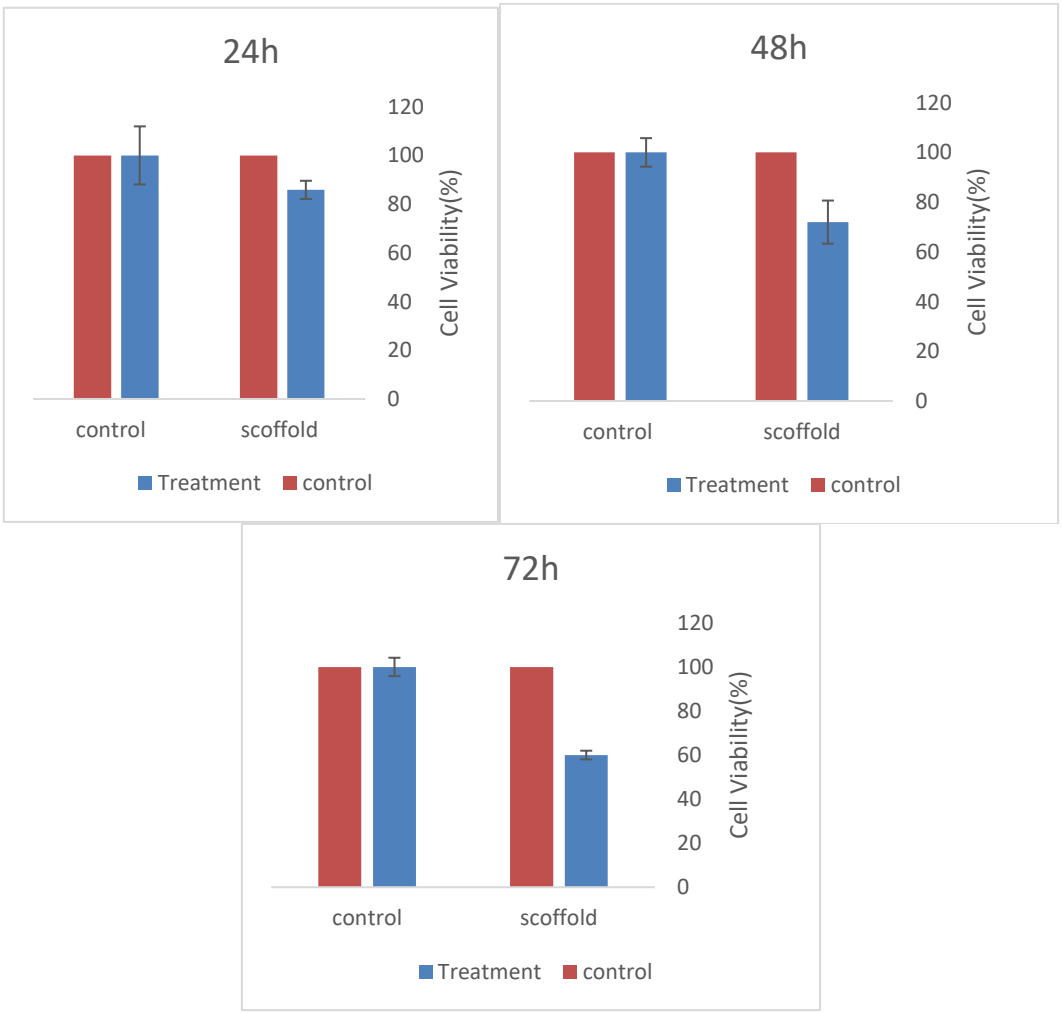

Fig 3: The viability of L929 human fibroblasts while incubating with the scaffolds for 24, 48 and 72 hours

3.1.2 Alkaline Phosphatase Activity (ALP)

Alkaline phosphatase is a cell membrane-associated enzyme which its intracellular activity is the main indicator of osteoblastic differentiation [29]. The main effects of ALP are the regulation of phosphate metabolism and down-regulation of osteoblast differentiation inhibitors. The expression and activity of ALP reduce after the beginning of mineralization which occurs at the later stages of osteoblast differentiation [30]. Bioactive materials such as ES-HA have positive impact on the degree of OSTEOBLAST-LIKE HOS proliferation and differentiation. The ALP activity of OSTEOBLAST-LIKE HOS cells cultured on polystyrene plates and GelMa/ES-HA scaffold samples at 6 days is shown in Fig. 4,5. ALP activity of the cells grown on scaffold samples was significantly higher than that of polystyrene plates under the same condition (p <0.05). The significantly higher ALP activity of OSTEOBLAST-LIKE HOS osteoblast

cells cultured on GelMa/ES-HA scaffold compared to the control groups, the cells cultured on the polystyrene plates confirmed that the scaffold samples were highly bioactive because they stimulated the early differentiation of osteoblastic cell.

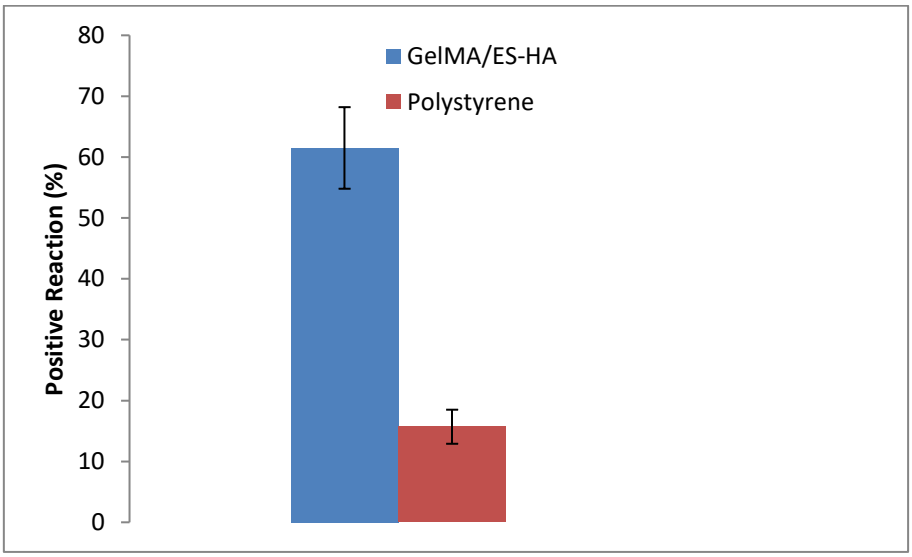

Fig 4: ALP activity of OSTEOBLAST-LIKE HOS cells cultured on GelMa/ES-HA scaffold and polystyrene plates after 6 days. The values are represented as the mean ± standard deviation of three replicates.

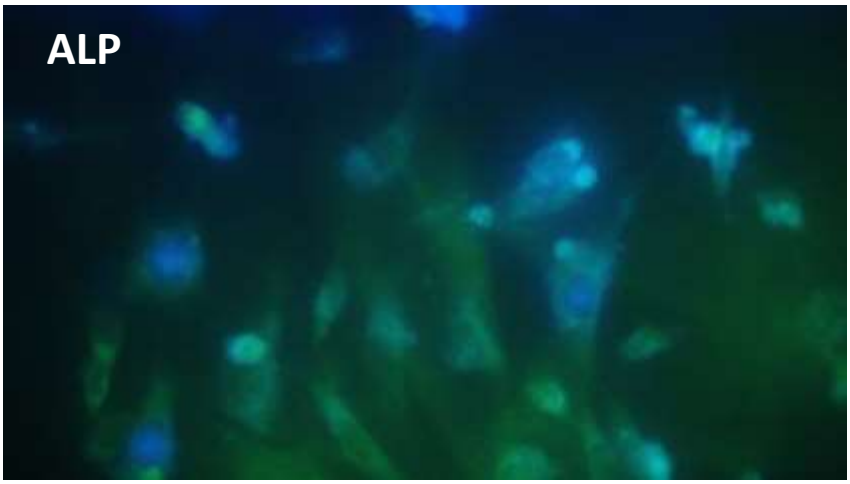

Fig 5: Fluorescence microscopy images of stained OSTEOBLAST-LIKE HOS cells after culturing for 6 days on the GelMA/ES-HA scaffolds. Calcein AM stained live cells green.

The significantly higher ALP level of cell cultured on the GelMa/ES-HA composite indicated that the addition of HA played a positive role in enhancing osteoblastic cell activity. Previously, the authors observed the positive role of calcium phosphates in enhancing ALP activity by osteoblast-like cells (MG63 and HOS) in a series of systems, such as bulk ceramics, porous scaffolds, and coatings [31]. In practice, not only the physical status, such as roughness and morphology, but also the chemical composition and ionic release of materials affect the cellular responses [32]. The rough surface created by the HA addition should affect the ALP activity of cells adversely, because the authors previously observed in a TiO_2-treated Ti system that a roughness increase reduced the ALP levels of osteoblast-like cells (MG63 and HOS). Moreover, the rougher surface was reported to result in down-regulation of ALP expression by osteoblast-like and human bone cells [33]. In this respect, even with the rougher surface in the GelMa/ES-HA composites affecting the ALP expression unfavorably, the up-regulation in ALP activity should be attributed to the ionic interactions between the bioactive HA and cells. To confirm the enhanced cell functionality, along with the intracellular assessment (ALP assay), the quantification of the secretion of bone-associated extracellular matrix proteins (osteocalcin) by the cells was also undertaken.

3.1.3 Osteocalcin secretion

Osteocalcin synthesis was also investigated as a parameter of osteoblast differentiation. Osteocalcin, a noncollageneous matrix protein, which is composed of two glutamic acid residues has a high affinity for Calcium and is known to inhibit the growth of apatite crystal both *in vitro* and *in vivo* [34]. Osteocalcin synthesis occurs during the late stages of osteoblast differentiation. Osteocalcin is a marker of mature osteoblastic cells (e.g. osteocytes), which actively produce mineralized tissue [35].

Osteocalcin synthesis for the cells cultured on the GelMa/ES-HA scaffold was significantly higher than on the polystyrene plate after 6 days of culture (Fig 6,7). The results of ALP activity and osteocalcin synthesis suggest that the bioactive GelMa/ES-HA scaffold improved the development of a mature osteoblast phenotype.

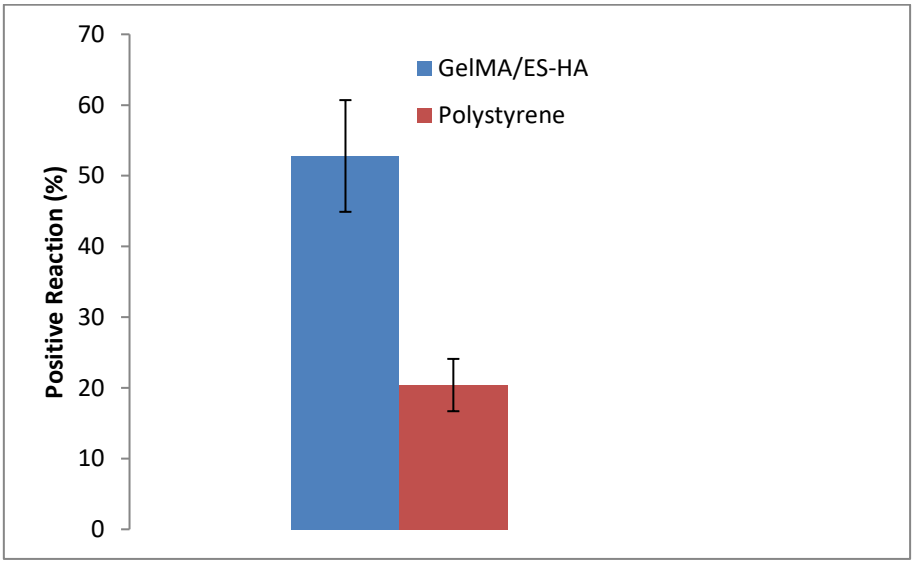

Fig 6: Osteocalcin synthesis of OSTEOBLAST-LIKE HOS cells cultured on GelMa/ES-HA scaffold and polystyrene plates after 6 days. The values are represented as the mean ± standard deviation of three replicates.

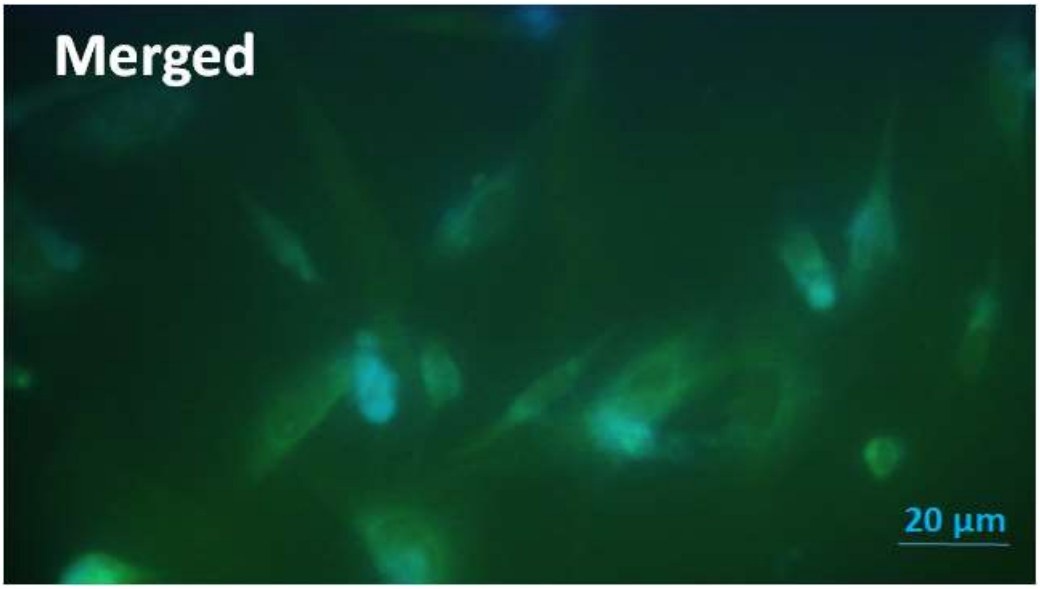

Fig 7: Fluorescence microscopy images of stained OSTEOBLAST-LIKE HOS cells after culturing for 3 days on the GelMA/ES-HA scaffolds. Calcein AM stained live cells green and ethidium homodimer-1 stained the nuclei of dead cells red.

The results of ALP activity and osteocalcin synthesis suggest that the bioactive GelMa/ES-HA scaffold improved the development of a mature osteoblast phenotype. At least from these findings on enhanced *in vitro* osteoblastic cell activity and preliminary mechanical properties, the GelMa/ES-HA scaffold is suggested to be applicable as a temporary hard tissue regenerative. Aparnathi & Patel [36] also showed that Canine Adipose-Derived Stem Cells (cADSCs) encapsulated in 5% GelMA porous scaffold demonstrated best morphology and were differentiated osteogenically. Osteogenic differentiation was affirmed by the presence of osteo-specific gene expression by reverse transcriptase PCR in addition to von Kossa staining of the construct.

This concept was further supported by the observation of discrete mineralized bone nodules in osteoblast cultures growing on the bioactive GelMa/ES-HA scaffold. Bone nodules consist of differentiated osteoblasts, extracellular matrix, and associated minerals, and their formation characterizes a late stage of osteoblast differentiation. Several lines of evidence suggest that their presence is a good index of osteogenesis *in vivo* [37].

3.1.4 SEM observation of cell cultured on the scaffold

Figure 8 (a-d) shows the SEM micrographs of the OSTEOBLAST-LIKE HOS cells grown on the GelMA/ES-HA scaffold after culturing for 3 days. The cells grew favorably on the surface of scaffold or between its pores even though the morphology of pores was complex. Several calcium depositions are also seen in the SEM micrographs.

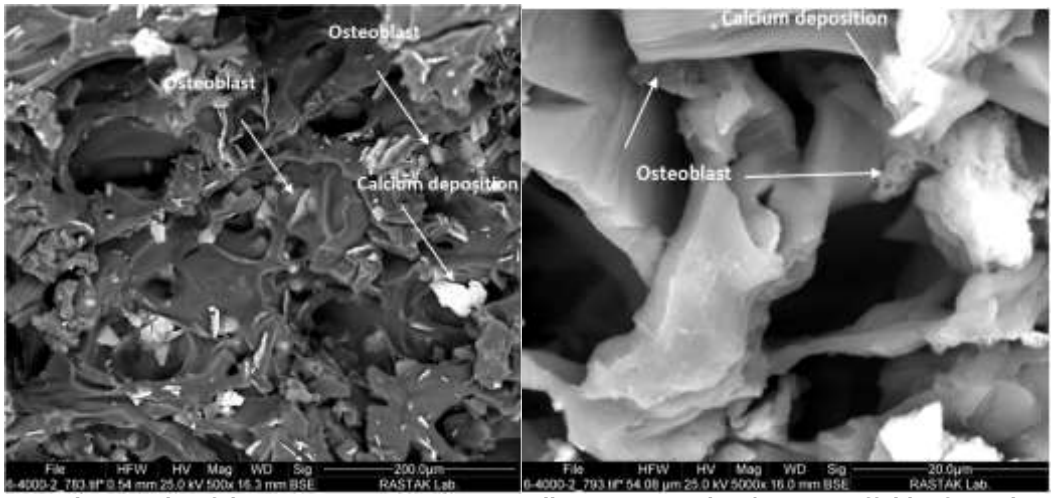

Fig 8: SEM micrographs of the OSTEOBLAST-LIKE HOS cells grown on GelMA/ES-HA scaffolds after culture for 3 days

3.2 In vivo studies

3.2.1 Histopathological Evaluation

Evaluation of bone healing in 7 days post-surgery, showed the defect area filled by delicate and intertwined bone trabeculae. The neoformed trabeculae contained large osteocytes and were surrounded by cuboid osteoblasts in all specimens, which disagreed with histological findings of the present study at 7 days duration which showed matrix deposition filled with large numerous osteocytes and rimmed by osteoblasts, no obvious trabecular formation could be seen. The histological examination of bone sections showed deposition of osteoid bone in all studied groups after 1-week and immature bone spicules rimmed by osteoblasts were observed more clearly in experimental groups. Significant osteoid matrix synthesis and mineralization accelerated was by early cell differentiation.

A small flattened and inactive osteoblasts were detected overlying the immature bone surfaces in the histological observations of defects at 1-week period. The number of osteoblasts as mean values increased during the transition from the 1, 4 to 8 and 12-weeks of healing intervals among all groups. It could be explained by the direct action of applied materials on the differentiating and maturation of osteoblasts accelerating rate of matrix deposition and its corresponding calcification, where osteocytes were embedded which also showed increasing mean values with time among groups.

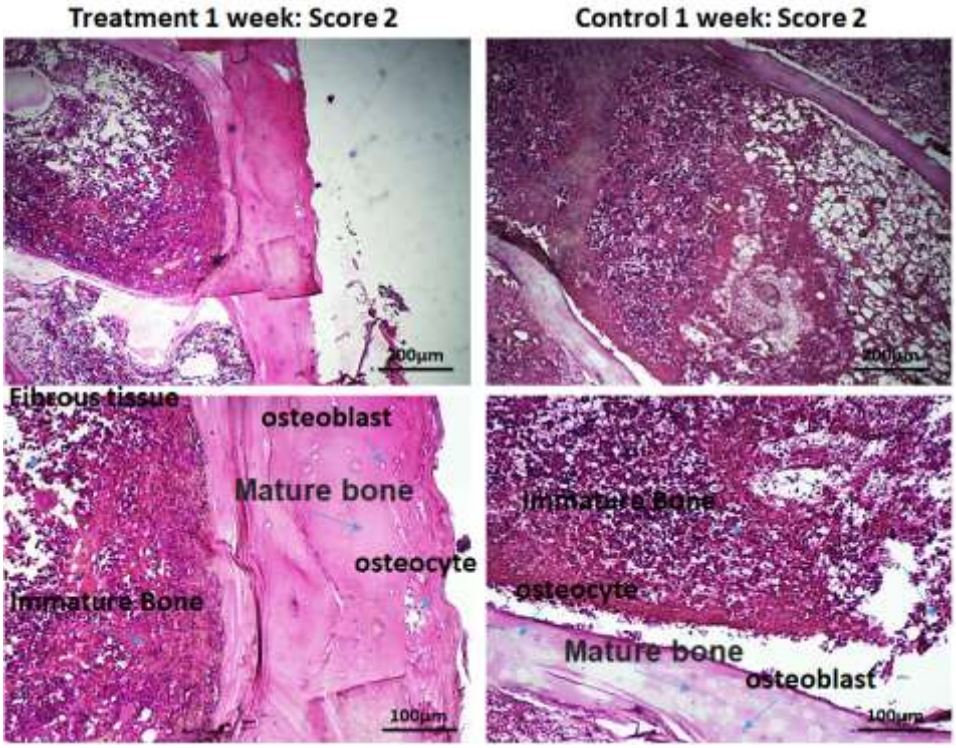

Fig 9: H&E images of tissue sample in treatment group and control group one week post-surgery

As seen in Fig 9, collagen fibers in these groups (treatment and control group after week 1) are arranged irregularly in different directions according to the images. Blood cells and osteoblast cells, are oriented on these collagens. The boundary between the mature bone and the area where the collagen or fibrosis tissue is immature bone or woven bone. In the 1w group ,there is amount of fibrosis tissue in which cellular foci are formed and enclosed within the collagen fibers. The border between the healing point and the normal bone area is clearly visible.

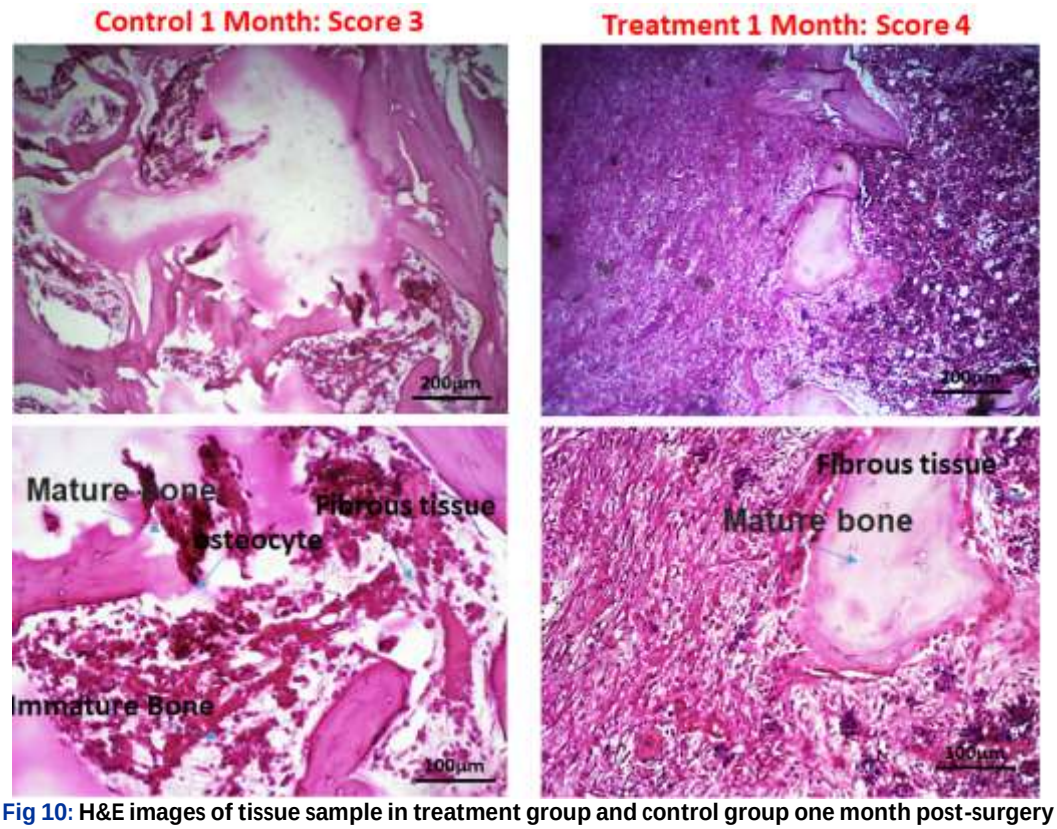

Fig 10: H&E images of tissue sample in treatment group and control group one month post-surgery

Collagen fibers in this group are arranged irregularly in different directions according to the images. Blood cells and osteoblast cells, are oriented on these collagens. The boundary between the mature bone and the area where the collagen or fibrosis tissue is immature bone or Woven bone.

In the 1 Month treatment group ,there is amount of fibrosis tissue in which cellular foci are formed and enclosed within the collagen fibers. The border between the healing point and the normal bone area is clearly visible (Fig 10).

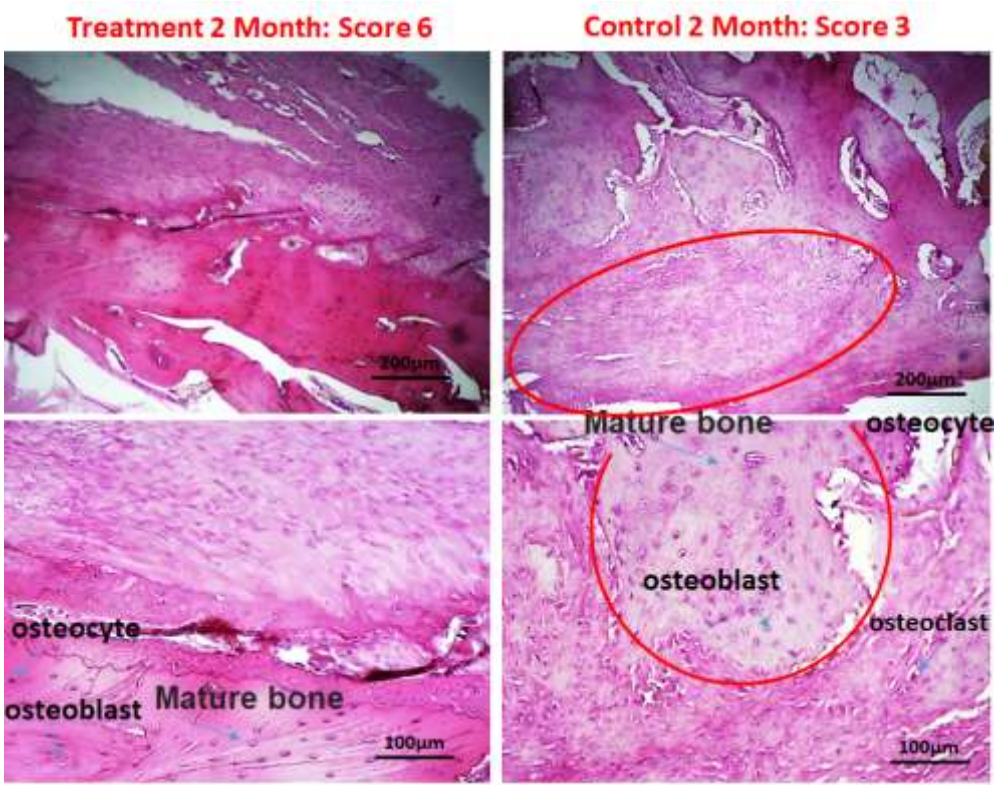

Fig 11: H&E images of tissue sample in treatment group and control group 2 months post-surgery

Collagen fibers orientation, Blood cells and osteoblast cells, The boundary between the mature bone and the area where the collagen or fibrosis tissue in the 2 month group in comparison with control group showed a elevated score. In damage area much of fibrosis tissue have filled empty spaces and a little immature bone in some area near the native bone have produced. The border between the healing point and the normal bone area is clearly visible, but disruption was seen in fibrosis tissue near damage area (Fig 11).

The local metabolic activity of bone cells have been seen in this group in fibrous tissue area. Collagen organization and the appearance of woven bone between collagen fiber have been observed more than 1w group, however, vary as a function of age. Age-related changes in bone architecture can be easily observed using samples of different simple in this groups but totally immature bone is produced more than half of tissue and have filled fibrous tissue area in border of mature and immature bone.

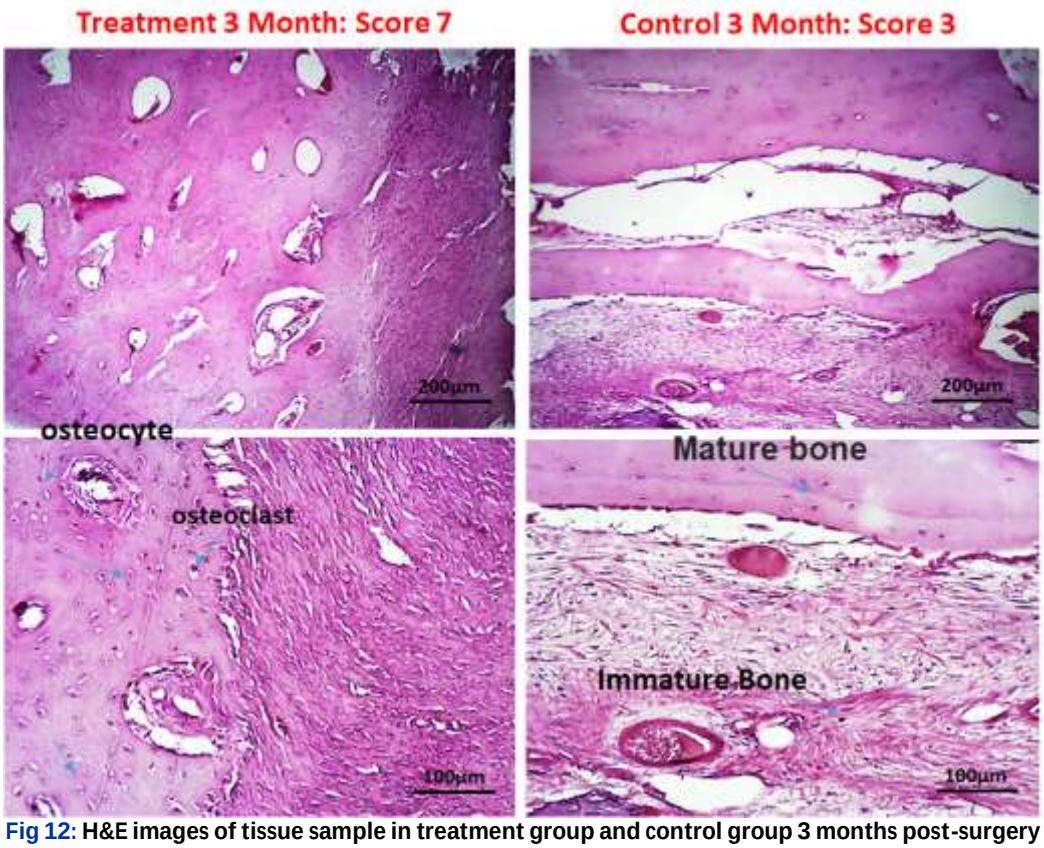

Fig 12: H&E images of tissue sample in treatment group and control group 3 months post-surgery

Collagen fibers orientation, Blood cells and osteoblast cells, The boundary between the mature bone and the area where the collagen or fibrosis tissue in the 3M group in comparison with other experimental groups contain 2M, 1M and 1w groups showed a high score in healing process and more half of tissue in near damage are was filled by fibrous connective tissue (Fig 12, 13).

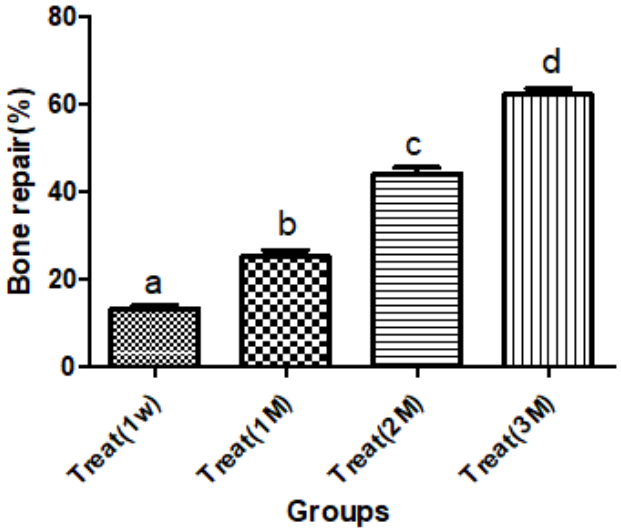

Fig 13: The percentages of bone repair in treatment groups one week, 1, 2 and 3 months post-surgery

3.2.2 Cell population in tissue samples

Osteocyte cell count

The population of Osteocytes in 1 week control and treatment groups was similar, 2433±4.1 and 25.33±1.15, respectively (Fig 14 a). However, population of Osteocytes in 1, 2 and 3 months treatment group was significantly higher than the control groups (Fig 14 b,c,d). The population of Osteocytes in 1, 2 and 3 months control groups was 23.00, 22.67, 23.00, respectively; while its value in treatment groups (1, 2 and 3 months) was 30.67, 36.33, 40.00, respectively.

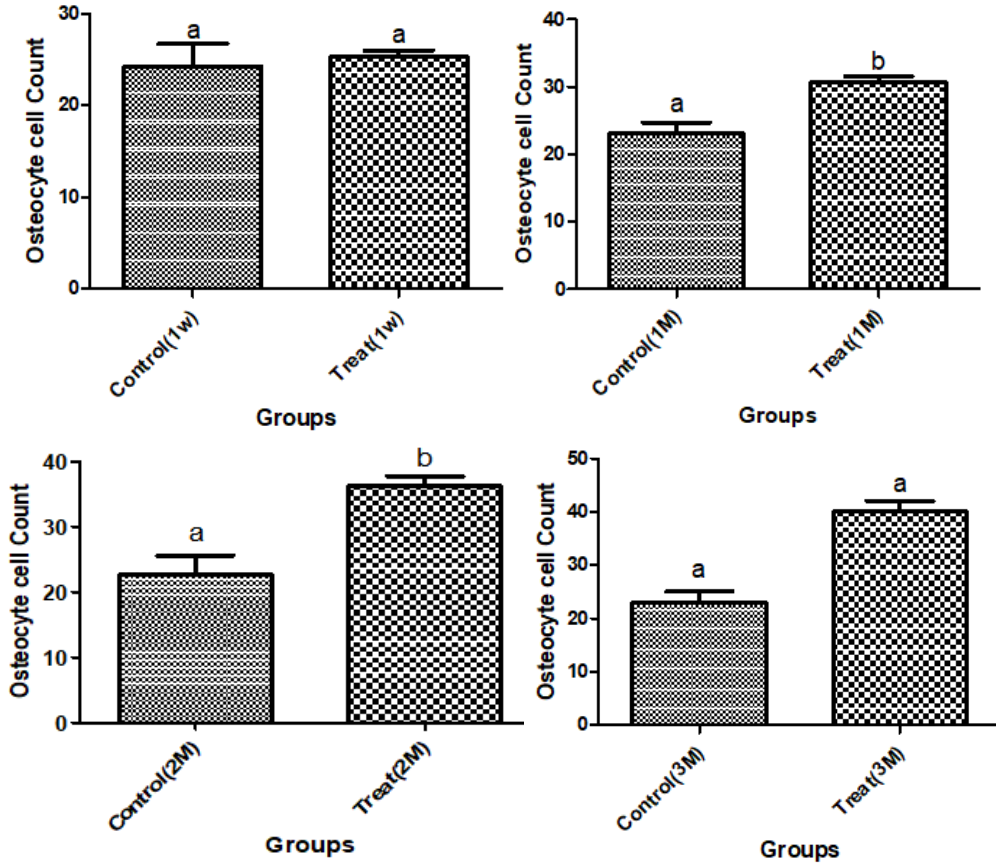

Fig 14: Osteocyte cell count in Treatment and control group a) one week, b) 1 month, c) 2 month, d) 3 month post-surgery

The Osteocyte cell count in treatment groups increased over time (Fig 15). Osteonectin production in 2 and 3 months treatment groups (36.33 and 40.00) was significantly higher than that in 1 week (25.33) and 1 month (30.67) treatment groups ($p< 0.05$). Also, the difference between Osteocyte cell count in 3 months treatment group and 1 month treatment group was significant ($p< 0.05$).

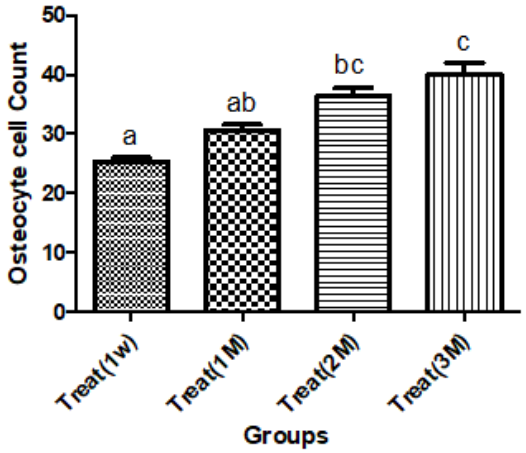

Fig 15: Osteocyte cell count in Treatment groups 1 week, 1, 2 and 3 months post-surgery

Osteoblast cell count

The population of Osteoblasts in 1 week and 1 month control and treatment groups was similar, respectively (Fig 16 a,b). However, population of Osteoblasts in 2 and 3 months treatment groups was significantly higher than the control groups (Fig 16 c,d). The population of Osteoblasts in 2 and 3 months control groups was 17.00, 17.67, respectively; while its value in treatment groups (1, 2 and 3 months) was 22.33, 25.00, respectively.

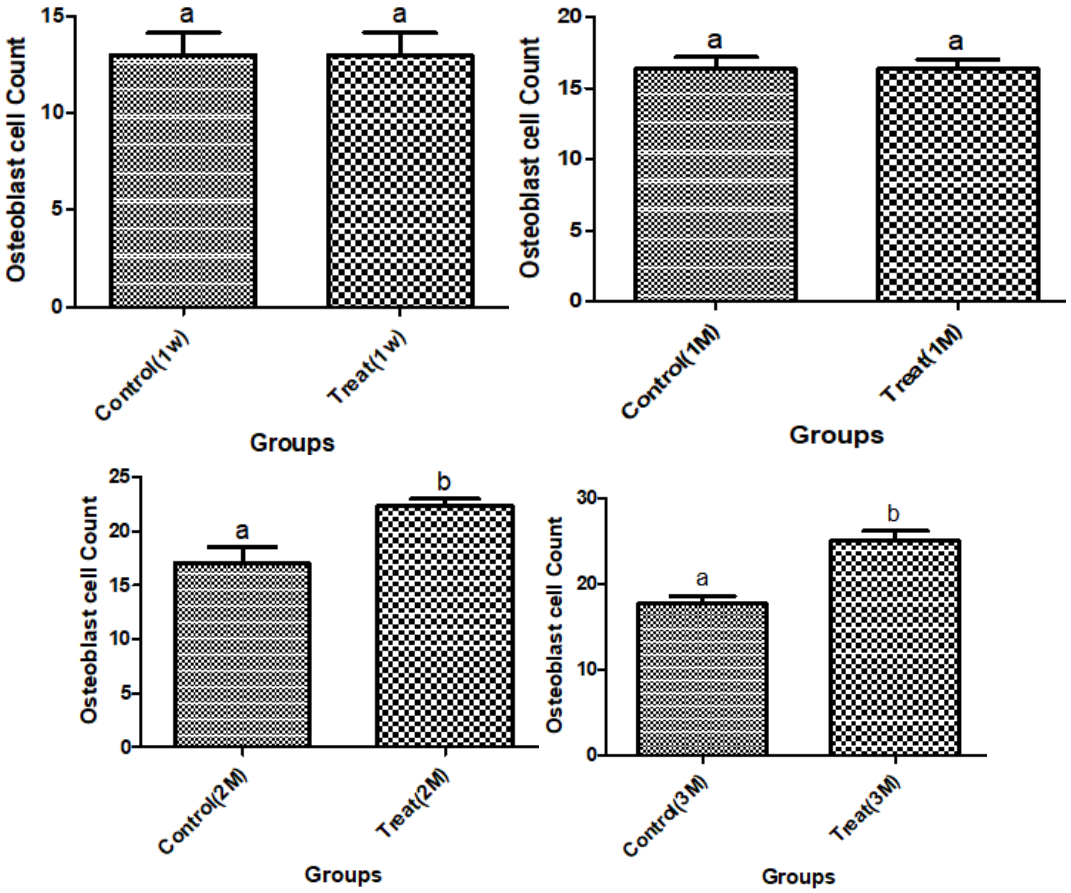

Fig 16: Osteoblast cell count in Treatment and control group a) one week, b) 1 month, c) 2 month, d) 3 month post-surgery

The Osteoblast cell count in treatment groups increased over time (Fig 17). Osteoblast cell count in 2 and 3 months treatment groups (22.33 and 25.00) was significantly higher than that in 1 week (13.00) and 1 month (16.33) treatment groups ($p< 0.05$). The difference between Osteoblast cell count in 3 months treatment group and 2 month treatment group was insignificant ($p> 0.05$).

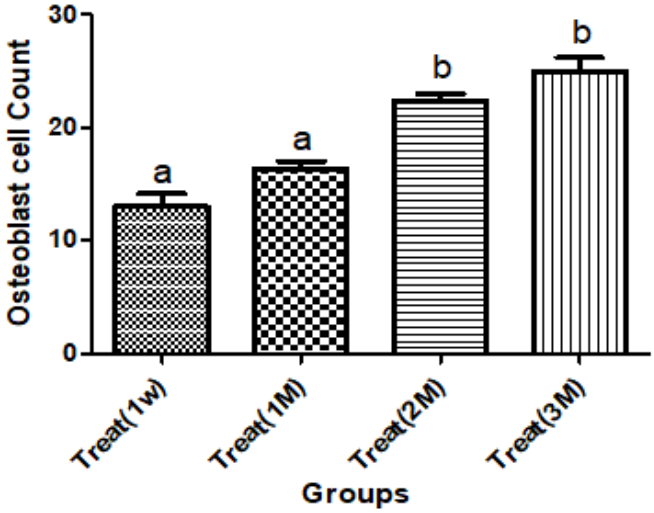

Fig 17: Osteoblast cell count in Treatment groups 1 week, 1, 2 and 3 months post-surgery

Significant increase in the cell number for the cells cultured on the GelMa/ES-HA scaffolds implicated that the scaffolds provided better support for bone cell adhesion and proliferation. The better support of the GelMa/ES-HA scaffolds for bone cell culture should be due to the presence of HA, a known osteoconductive material, and the excellent hydrophillicity of GelMA. Similar to our results, Chuenjitkuntaworn et al. [38] showed that PCL/HA composite scaffolds improved the adhesion and proliferation of human primary bone cells. In addition, the presence of HAp particles within the scaffolds may also facilitate specific adsorption of serum proteins that could help regulate the adhesion and proliferation of the cells.

Osteoclast cell count

The population of Osteoclast in 1 week control and treatment groups was similar, 5.000±1.0 and 4.66±0.5, respectively (Fig 18 a). However, population of Osteocytes in 1, 2 and 3 months treatment group was lower than the control groups (Fig 18 b,c,d). The population of Osteocytes in 1, 2 and 3 months control groups was 5.00, 3.66, 2.66, respectively; while its value in treatment groups (1, 2 and 3 months) was 3.33, 2.66, 1.33, respectively.

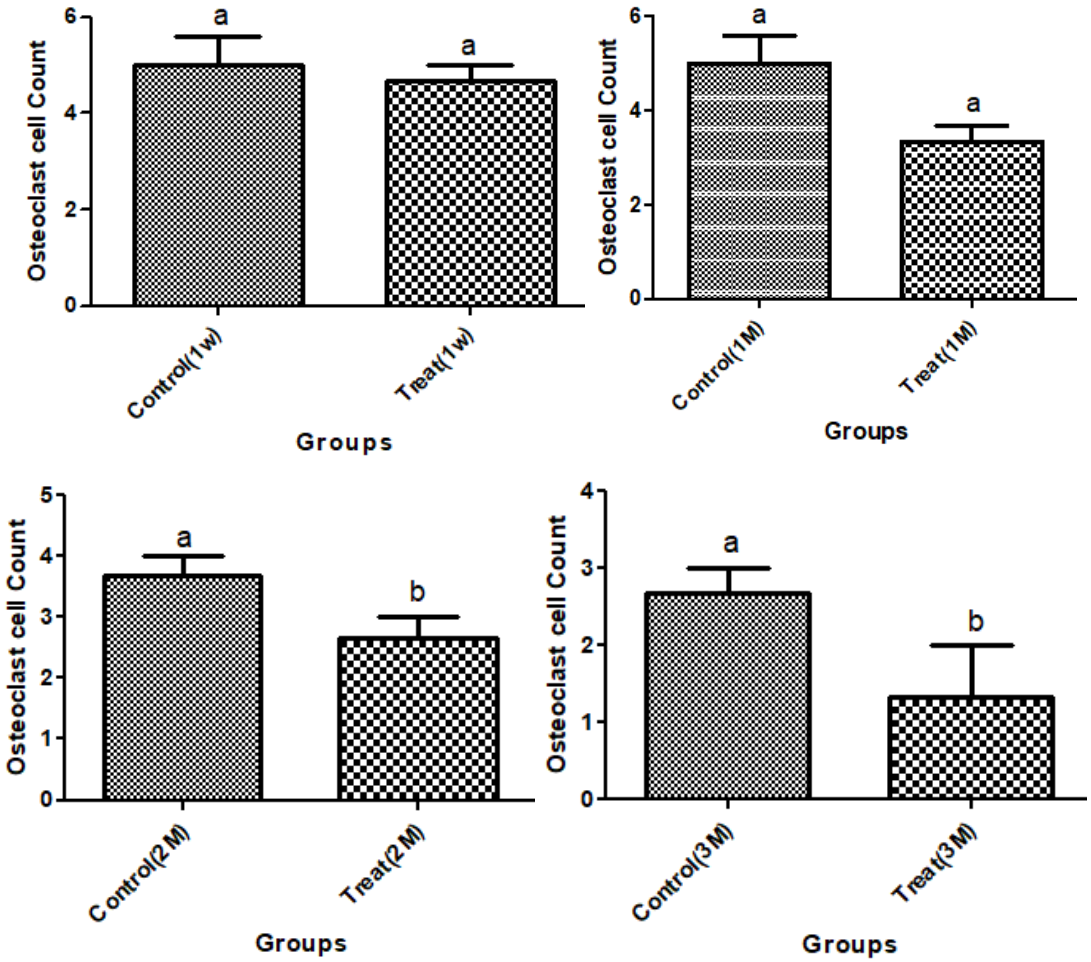

Fig 18: Osteoclast cell count in Treatment and control group a) one week, b) 1 month, c) 2 month, d) 3 month post-surgery

The Osteoclast cell count in treatment groups decreased over time (Fig 19). Osteoclast cell count in 2 and 3 months treatment groups (2.66 and 1.33) was significantly lower than that in 1 week (4.66) treatment groups ($p< 0.05$). The difference between Osteoclast cell count in 3 months treatment group and 1 month treatment group (3.33) was also significant ($p> 0.05$).

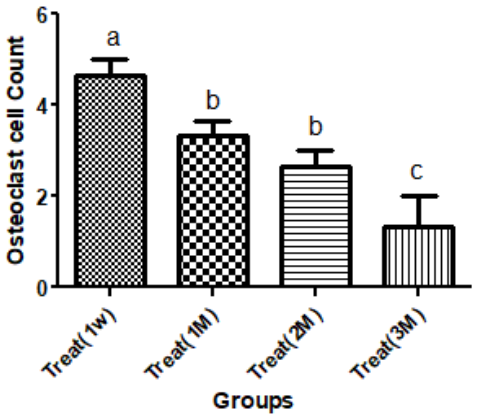

Fig 19: Osteoclast cell count in Treatment groups 1 week, 1, 2 and 3 months post-surgery

3.2.3 Immuno-histomorphometry and fluorescent characteristics of tissue samples

3.2.3.1 Osteocalsin production

Osteocalsin production in 1 week control and treatment groups was similar, 12.52±1.5 and 12.93±2.6, respectively. However, Osteocalsin production in 3 months treatment group was significantly higher than the 3 months control group (Fig 20). Osteocalsin production in 1, 2 and 3 months control groups was 14.99, 15.78, 17.49, respectively; while its value in treatment groups (1, 2 and 3 months) was 16.99, 19.80, 34.26, respectively.

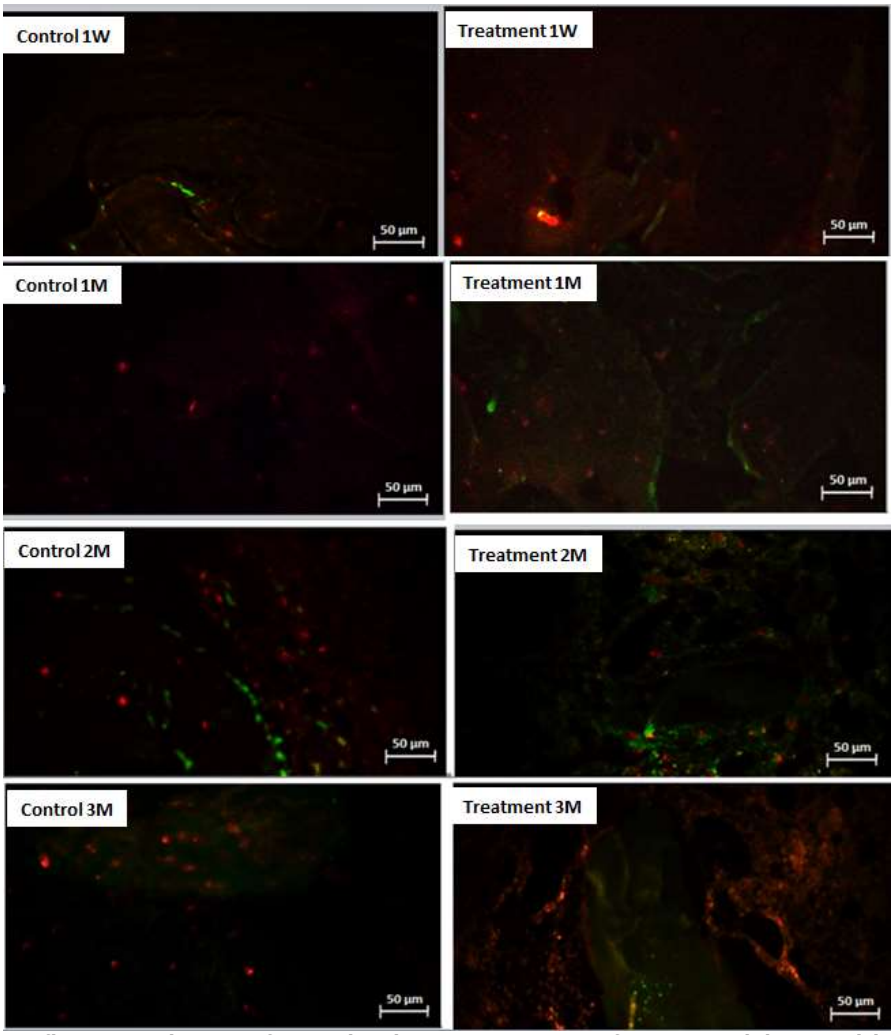

Fig 20: Immuno-flourescent images of control and treatment groups after one week (Osteocalsin production)

The Osteocalsin production in treatment groups increased over time (Fig 21). Osteocalsin production in 3 months treatment group (34.26) was significantly higher than that of 1 week (12.93) and 1 month (16.99) and 2 month (19.84) treatment groups ($p< 0.05$).

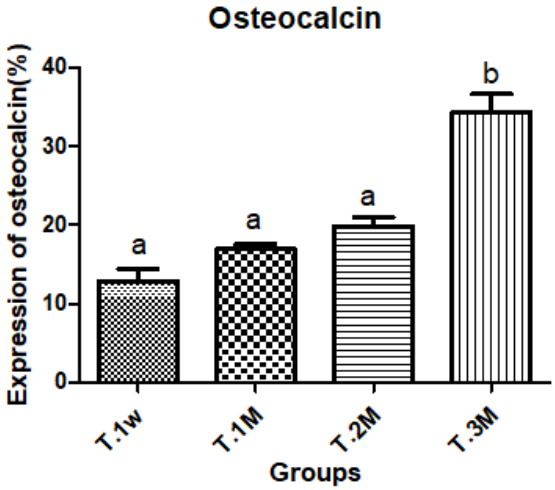

Fig 21: The percentages of Osteocalsin production in treatment groups after one week, 1, 2, 3 months

3.2.3.2 Osteopointin production

After 1 week the production of Osteopointin in control and treatment groups was similar, 12.95±1.9 and 11.25±3.9, respectively (Fig 22). However, over time Osteopointin production in treatment groups significantly increased compared to control groups (Fig 22). Osteopointin production in 1, 2 and 3 months control groups was 14.70, 13.64, 14.73, respectively; while its value in treatment groups (1, 2 and 3 months) was 17.73, 27.70, 42.43, respectively.

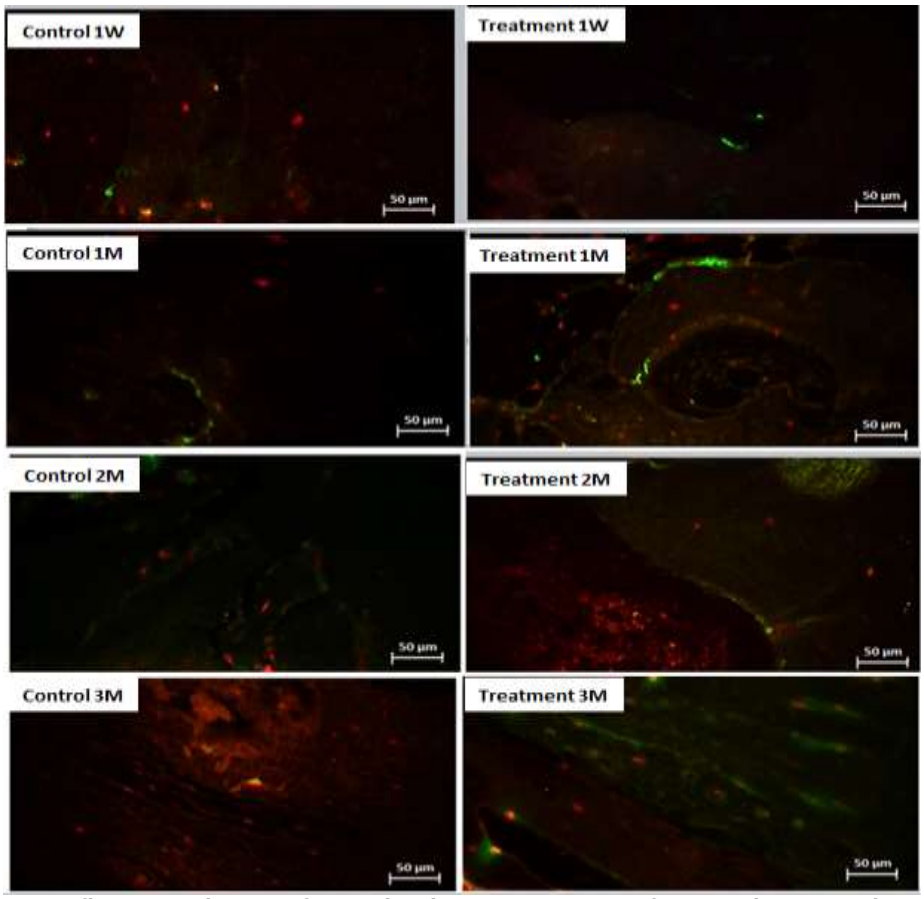

Fig 22: Immuno-flourescent images of control and treatment groups after 1 week, 1, 2, 3 M (Osteopointin production)

The Osteopointin production in treatment groups increased over time (Fig 23). Osteonectin production in 2 and 3 months treatment groups (27.70 and 42.43) was significantly higher than that in 1 week (11.25) and 1 month (17.73) treatment groups ($p< 0.05$). The difference between Osteonectin production in 3 months treatment group and the treatment groups after 1 and 2 months was also significant ($p< 0.05$).

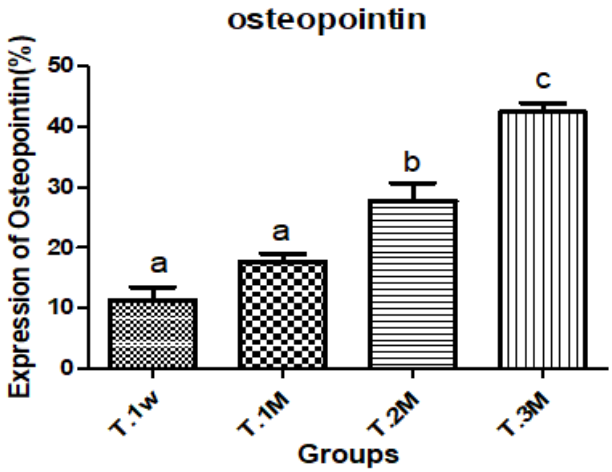

Fig 23: The percentages of Osteopointin production in treatment groups after 1 week, 1, 2, 3 months

3.2.3.3 Osteonectin production

After 1 week the production of Osteronectin in control and treatment groups was similar, 17.65±2.3 and 16.90±3.9, respectively (Fig 24). However, over time Osteronectin production in treatment groups significantly increased compared to control groups (Fig 24). Osteronectin production in 1, 2 and 3 months control groups was 17.37, 14.9, 14.50, respectively; while its value in treatment groups (1, 2 and 3 months) was 25.66, 29.16, 34.26, respectively.

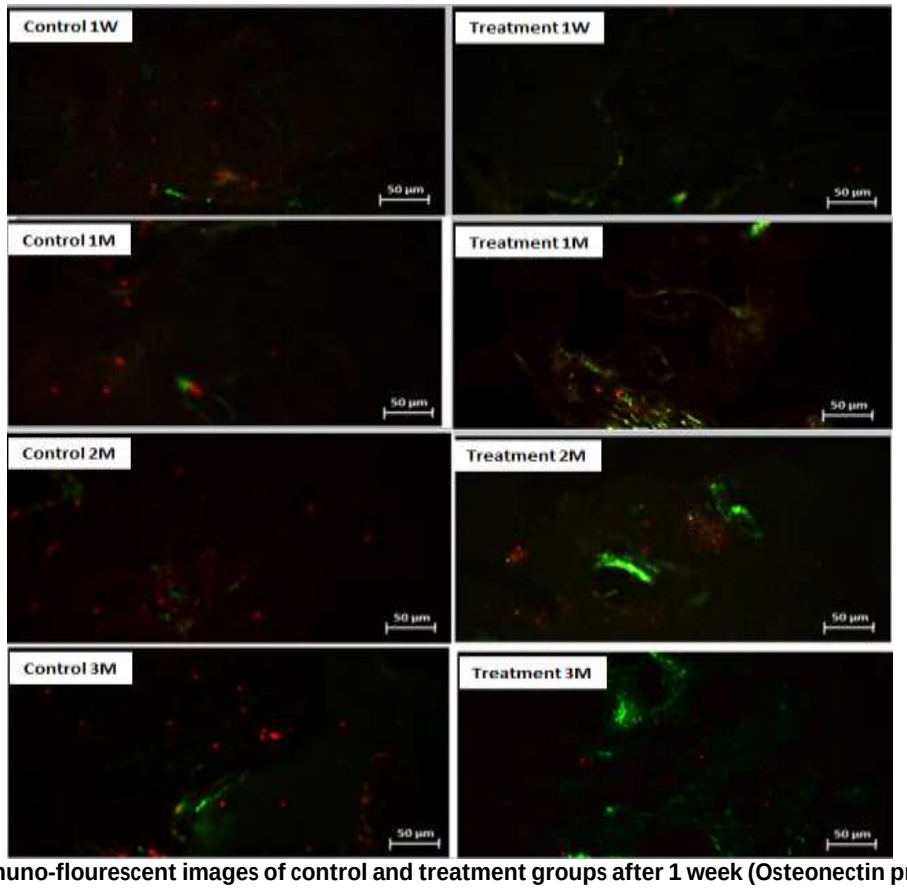

Fig 24: Immuno-flourescent images of control and treatment groups after 1 week (Osteonectin production)

The Osteonectin production in treatment groups increased over time (Fig 25). Osteonectin production in 1, 2 and 3 months treatment groups (25.66, 29.16 and 34.26) was significantly higher than that in 1 week treatment groups (16.90, $p< 0.05$). Also, the difference between Osteonectin production in 3 months treatment group and 1 month treatment group was significant ($p< 0.05$).

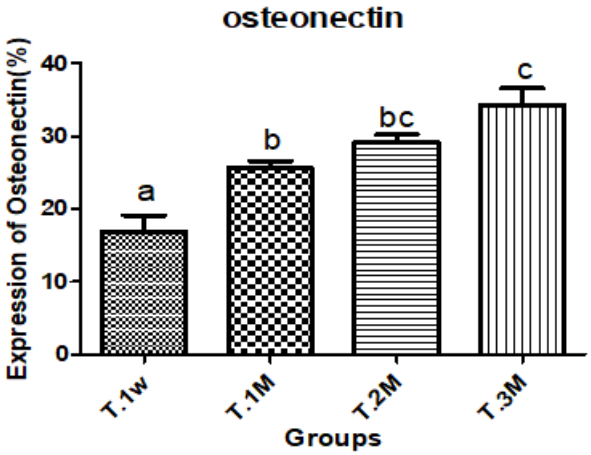

Fig 25: The percentages of Osteonectin production in treatment groups after 1 week, 1, 2, 3 months

Osteocalsin, Osteopointin and Osteronectin production in 1 week control and treatment groups was similar. However, over time their production in treatment groups significantly increased compared to control groups. Furthurmore, production of these osteogenic factors in treatment groups significantly increased over time. As mentioned before, the good osteoinductive propersites of the GelMa/ES-HA scaffolds could be attributed to the presence of osteoconductive HA particles, and the also excellent hydrophillicity of GelMA and highly porous structure and the suitable degradation rate of GelMa/ES-HA composite scaffold.

Altogether, the observations prove that the GelMA/ES-HA composite scaffolds can act as excellent bone tissue engineering candidate which promote great osteogenesis in defected bone tissue and may have great potential in future clinical applications.

CONCLUSION

GelMa/ES-HA composite scaffold was sucessfully fabricated via freeze-drying process. First, the HA powder was obtained from eggshell waste material. The *in vitro* cellular responses to the GelMa/ES-HA composite scaffold were assessed via cell growth and proliferation (MTT assay), alkaline phosphatase activity and osteocalcin production using osteoblast-like HOS cells. The effect of GelMa/ES-HA scaffold on bone regrowth and regeneration was evaluated *in vivo* on a nine months old sheep.

The cytotoxicity of composite scaffolds was low after 24 h incubations (The viability of cells was above 85%). However, the cell viability decreased over time (71.9% after 48 h and 60.0% after 72 h). ALP activity of the cells grown on scaffold samples was significantly higher than that of polystyrene plates under the same condition ($p <0.05$). Also, ALP activity of scaffold samples increased over time. Osteocalcin synthesis for the cells cultured on the GelMa/ES-HA scaffold was significantly higher than on the polystyrene plate after 6 days of culture. The results of ALP activity and osteocalcin synthesis suggest that the bioactive GelMa/ES-HA scaffold improved the development of a mature osteoblast phenotype. SEM micrographs of the HOS cells grown on the scaffold after culturing for 3 days confirmed the favorable cells growth of cells on the surface of scaffold or between its pores and also formation of calcium deposits.

The histological examination of bone sections showed deposition of osteoid bone in all studied groups after 1-week and immature bone spicules rimmed by osteoblasts were observed more clearly in treatment groups. Significant osteoid matrix synthesis and mineralization accelerated was by early cell differentiation. The number of osteocytes and osteoblasts as mean values increased during the transition from the 1, 4 to 8 and 12-weeks of healing intervals among treatment groups. While, the Osteoclast population in treatment groups decreased over time. The production of Osteocalsin, Osteopointin and Osteronectin in treatment groups significantly increased over time ($p< 0.05$). Furthermore, the difference between Osteocalsin, Osteopointin and Osteonectin production in all treatment group and control groups was significant ($p< 0.05$) except for the 1 week groups. The maximum Osteocalsin, Osteopointin and Osteronectin production belonged to 3 months treatment group which were 34.26, 42.43 and 34.26, respectively; which this values for 3 months control groups were 17.49, 14.73 and 14.50.

The results of this study showed that the novel GelMa/ES-HA composite scaffold is a bioactive, biocompatible, biodegradable bone graft with desired mechanical and swelling properties and excellent potential for enhancing bone regeneration proces which could serve as a promissing candidate for bone and dental tissue engineering applications.

CONFLICT OF INTEREST: Nil

REFERENCES

1. Lanza, R., Langer, R., Vacanti, J. P., & Atala, A. (Eds.). (2020). *Principles of tissue engineering*. Academic press.
2. Kashi, Mana, et al. "Green synthesis of degradable conductive thermosensitive oligopyrrole/chitosan hydrogel intended for cartilage tissue engineering." International journal of biological macromolecules 107 (2018): 1567-1575.
3. Hutmacher, Dietmar W. "Scaffolds in tissue engineering bone and cartilage." *Biomaterials* 21.24 (2000): 2529-2543.
4. Baghbani, F., et al. "Biological response of biphasic hydroxyapatite/tricalcium phosphate scaffolds intended for low load-bearing orthopaedic applications." Advanced Composites Letters 21.1 (2012): 096369351202100102.
5. Gholizadeh, Shayan, et al. "Preparation and characterization of novel functionalized multiwalled carbon nanotubes/chitosan/β-Glycerophosphate scaffolds for bone tissue engineering." International journal of biological macromolecules 97 (2017): 365-372.
6. Srouji, Samer, Tali Kizhner, and Erella Livne. "3D scaffolds for bone marrow stem cell support in bone repair." (2006): 519-528.
7. Qasim, Muhammad, Dong Sik Chae, and Nae Yoon Lee. "Advancements and frontiers in nano-based 3D and 4D scaffolds for bone and cartilage tissue engineering." *International journal of nanomedicine* 14 (2019): 4333.
8. Mewhort, Holly EM, et al. "Bioactive extracellular matrix scaffold promotes adaptive cardiac remodeling and repair." *JACC: Basic to Translational Science* 2.4 (2017): 450-464.
9. Baptista, Leandra Santos, et al. "Adult stem cells spheroids to optimize cell colonization in scaffolds for cartilage and bone tissue engineering." *International journal of molecular sciences* 19.5 (2018): 1285.
10. Szafron, Jason M., et al. "Optimization of tissue-engineered vascular graft design using computational modeling." *Tissue Engineering Part C: Methods* 25.10 (2019): 561-570.
11. Chung, Liam, et al. "Key players in the immune response to biomaterial scaffolds for regenerative medicine." *Advanced drug delivery reviews* 114 (2017): 184-192.
12. Asghari, Fatemeh, et al. "Biodegradable and biocompatible polymers for tissue engineering application: a review." *Artificial cells, nanomedicine, and biotechnology* 45.2 (2017): 185-192.
13. Ghalia, Mustafa Abu, and Yaser Dahman. "Biodegradable poly (lactic acid)-based scaffolds: synthesis and biomedical applications." *Journal of Polymer Research* 24.5 (2017): 74.
14. Ogueri, Kenneth S., et al. "Polymeric biomaterials for scaffold-based bone regenerative engineering." *Regenerative engineering and translational medicine* 5.2 (2019): 128-154.
15. Akilbekova, Dana, et al. "Biocompatible scaffolds based on natural polymers for regenerative medicine." *International journal of biological macromolecules* 114 (2018): 324-333.
16. Abbasian, Mojtaba, et al. "Scaffolding polymeric biomaterials: Are naturally occurring biological macromolecules more appropriate for tissue engineering?." *International journal of biological macromolecules* (2019).
17. Baghbani, Fatemeh, et al. "Synthesis, characterization and evaluation of bioactivity and antibacterial activity of quinary glass system (SiO 2–CaO–P 2 O 5–MgO–ZnO): in vitro study." Bulletin of Materials Science 36.7 (2013): 1339-1346.
18. Yue, Kan, et al. "Synthesis, properties, and biomedical applications of gelatin methacryloyl (GelMA) hydrogels." *Biomaterials* 73 (2015): 254-271.
19. Yin, Jun, et al. "3D bioprinting of low-concentration cell-laden gelatin methacrylate (GelMA) bioinks with a two-step cross-linking strategy." *ACS applied materials & interfaces* 10.8 (2018): 6849-6857.
20. Stratesteffen, Henrike, et al. "GelMA-collagen blends enable drop-on-demand 3D printablility and promote angiogenesis." *Biofabrication* 9.4 (2017): 045002.
21. Modaresifar, Khashayar, Afra Hadjizadeh, and Hassan Niknejad. "Design and fabrication of GelMA/chitosan nanoparticles composite hydrogel for angiogenic growth factor delivery." *Artificial cells, nanomedicine, and biotechnology* 46.8 (2018): 1799-1808.
22. Shin, Su Ryon, et al. "Reduced graphene oxide-gelMA hybrid hydrogels as scaffolds for cardiac tissue engineering." *Small* 12.27 (2016): 3677-3689.3
23. Sofi, Hasham S., et al. "Scaffolds fabricated from natural polymers/composites by electrospinning for bone tissue regeneration." *Cutting-Edge Enabling Technologies for Regenerative Medicine*. Springer, Singapore, 2018. 49-78.
24. Chen, Jiali, et al. "3D bioprinted multiscale composite scaffolds based on gelatin methacryloyl (GelMA)/chitosan microspheres as a modular bioink for enhancing 3D neurite outgrowth and elongation." *Journal of Colloid and Interface Science* (2020).
25. Zhuang, Tiantian, et al. "A GelMA/DECM/Nanoclay Composite Biomaterial Ink for Printing 3D Scaffolds for Primary Hepatocytes Cultivation." *Materials Letters* (2020): 128034.
26. Ramesh, S., et al. "Direct conversion of eggshell to hydroxyapatite ceramic by a sintering method." *Ceramics international* 42.6 (2016): 7824-7829.
27. Patil, Chandrashekhar K., et al. "Functional antimicrobial and anticorrosive polyurethane composite coatings from algae oil and silver doped egg shell hydroxyapatite for sustainable development." *Progress in Organic Coatings* 128 (2019): 127-136.
28. Fares, M. M., Sani, E. S., Lara, R. P., Oliveira, R. B., Khademhosseini, A., & Annabi, N. "Interpenetrating

network gelatin methacryloyl (GelMA) and pectin-g-PCL hydrogels with tunable properties for tissue engineering. " *Biomaterials science*, *6*(11) (2018): 2938-2950.

29. Tang, Ling, et al. "miR-144 promotes the proliferation and differentiation of bone mesenchymal stem cells by downregulating the expression of SFRP1." *Molecular medicine reports* 20.1 (2019): 270-280.
30. Whyte, M. P. (2018). Hypophosphatasia and how alkaline phosphatase promotes mineralization. In *Genetics of bone biology and skeletal disease* (pp. 481-505). Academic Press.
31. Peñarrieta-Juanito, G., Cruz, M., Costa, M., Miranda, G., Marques, J., Magini, R., ... & Silva, F. S. (2018). A novel gradated zirconia implant material embedding bioactive ceramics: Osteoblast behavior and physicochemical assessment. Materialia, 1, 3-14.
32. Baghbani, Fatemeh, et al. "Production and characterization of a Ag-and Zn-doped glass-ceramic material and in vitro evaluation of its biological effects." Journal of Materials Engineering and Performance 25.8 (2016): 3398-3408.
33. Anselme, K. (2000). Osteoblast adhesion on biomaterials. Biomaterials, 21(7), 667-681.
34. Zoch, Meredith L., Thomas L. Clemens, and Ryan C. Riddle. "New insights into the biology of osteocalcin." *Bone* 82 (2016): 42-49.
35. Hu, K., & Olsen, B. R. (2016). Osteoblast-derived VEGF regulates osteoblast differentiation and bone formation during bone repair. *The Journal of clinical investigation*, *126*(2), 509-526.
36. Aparnathi, Mansi K., and Jagdish S. Patel. "Biodegradable gelatin methacrylate gel as a potential scaffold for bone tissue engineering of canine adipose-derived stem cells." *Journal of stem cells* 11.3 (2016): 111.
37. Rumney, Robin MH, et al. "In vivo delivery of VEGF RNA and protein to increase osteogenesis and intraosseous angiogenesis." *Scientific reports* 9.1 (2019): 1-10.
38. Huang, Boyang, et al. "Polymer-ceramic composite scaffolds: The effect of hydroxyapatite and β-tri-calcium phosphate." *Materials* 11.1 (2018): 129.

Cite this article: Jodal Mohammedamim Ahmed. 2020. In Vitro and In Vivo Evaluation of Osteoconductive Properties of Novel GelMa / Egg Shell – Derived Calcium Phosphate Composite Scaffold. European Journal of Molecular & Clinical Medicine, 7(2), pp. 01 – 19, DOI: https://doi.org/10.31838/ejmcm.07.02.01